Title

mTORC2-mediated direct phosphorylation regulates YAP activity promoting glioblastoma growth and invasive characteristics

Journal

Neoplasia, 23(9)

ISSN

1522-8002

Authors

Holmes, Brent
Benavides-Serrato, Angelica
Saunders, Jacquelyn T
et al.

Publication Date

2021-09-01

DOI

10.1016/j.neo.2021.07.005

Peer reviewed

NEOPLASIA
www.neoplasia.com
Volume 23 Number xxx Month 2021 pp. 951–965

Original Research

mTORC2-mediated direct phosphorylation regulates YAP activity promoting glioblastoma growth and invasive characteristics ☆, ☆☆

Brent Holmes [1,6]; Angelica Benavides-Serrato [1,6]; Jacquelyn T. Saunders [1,6]; Sunil Kumar [5,6]; Robert N. Nishimura [2,6]; Joseph Gera [1,3,4,6,*]

[1] Departments of Medicine
[2] Neurology, David Geffen School of Medicine at UCLA
[3] Jonnson Comprehensive Cancer Center
[4] Molecular Biology Institute, University of California-Los Angeles, CL
[5] Department of Pharmaceutical and Biomedical Sciences, California Health Sciences University, Clovis, CL
[6] Department of Research & Development, Greater Los Angeles Veterans Affairs Healthcare System, Los Angeles, CL

Abstract

The Hippo and mTOR signaling cascades are major regulators of cell growth and division. Aberrant regulation of these pathways has been demonstrated to contribute to gliomagenesis and result in enhanced glioblastoma proliferation and invasive characteristics. Several crosstalk mechanisms have been described between these two pathways, although a complete picture of these signaling interactions is lacking and is required for effective therapeutic targeting. Here we report the ability of mTORC2 to directly phosphorylate YAP at serine 436 (Ser^{436}) positively regulating YAP activity. We show that mTORC2 activity enhances YAP transcriptional activity and the induction of YAP-dependent target gene expression while its ablation via genetic or pharmacological means has the opposite affects on YAP function. mTORC2 interacts with YAP via Sin1 and mutational analysis of serine 436 demonstrates that this phosphorylation event affects several properties of YAP leading to enhanced transactivation potential. Moreover, YAP serine 436 mutants display altered glioblastoma growth, migratory capacity and invasiveness both *in vitro* and in xenograft experiments. We further demonstrate that mTORC2 is able to regulate a Hippo pathway resistant allele of YAP suggesting that mTORC2 can regulate YAP independent of Hippo signaling. Correlative associations between the expression of these components in GBM patient samples also supported the presence of this signaling relationship. These results advance a direct mTORC2/YAP signaling axis driving GBM growth, motility and invasiveness.

Neoplasia (2021) 23, 951–965

Keywords: mTORC2, YAP, Signal transduction, Phosphorylation, Glioblastoma

Introduction

Glioblastomas are the most prevalent and deadly of nervous system tumors [1]. Current treatment of surgery, radiation and chemotherapy typically results in tumor resistance and patients succumb within ~ 12 months [2]. Several groups have now demonstrated overexpression of the mTORC2 defining component, Rictor, in several cancers leading to increased nucleation of mTORC2 and its hyperactivity in GBM [3-7]. Elevated mTORC2 activity has been demonstrated to promote GBM proliferation, migration and invasive cell characteristics [7].

The mechanistic target of rapamycin (mTOR) protein kinase exists in at least two functionally distinct complexes, mTORC1 and mTORC2, and integrates signal transduction cascades coordinating cell growth, nutrient status, autophagy and protein synthesis [8]. The mTORC1 and mTORC2 kinases both contain mTOR, mLST8 (GβL), Deptor and Tti1/Tel2 however,

* Corresponding Author.
E-mail address: jgera@mednet.ucla.edu (J. Gera).
☆ ☆ Funding: This work was supported, in whole or in part, by VA MERIT I01BX002665 and NIH R01CA217820 grants.
☆☆ ☆☆ Conflict of interest: The authors declare no competing financial interests
Received 11 May 2021; received in revised form 8 July 2021; accepted 12 July 2021

https://doi.org/10.1016/j.neo.2021.07.005

mTORC1 specifically contains Raptor and PRAS40, while mTORC2 contains Rictor, mSin1 and Protor [9]. The regulatory inputs governing mTORC1 activity have been extensively studied, however the mechanisms regulating mTORC2 activity are still unclear. mTORC2 activity is known to be regulated by PI3K signaling and growth factor receptor engagement [10]. Ribosomal association has also been shown to activate mTORC2 [11,12]. mTORC2 has been demonstrated to activate several downstream effectors, however its best characterized substrate is the phosphorylation of serine 473 of AKT within the hydrophobic turn motif leading to full activation of AKT [13]. A constitutively active variant of the epidermal growth factor receptor, EGFRvIII has been demonstrated to activate mTORC2 in addition to PTEN loss in GBM [14]. In an EGFR-PI3K driven *Drosophila* glial tumor system, mTORC2 activity was demonstrated to be required for tumor formation, and Rictor overexpression has been shown to be sufficient to induce gliomagenesis in transgenic mice [4, 15].

In concert with the mTOR pathway, the Hippo signaling cascade has emerged as a critical signaling pathway regulating cell growth, survival and conferring oncogenic properties, in addition to contributing to GBM proliferation, motility and invasiveness [16-18]. Following Hippo kinase activation (MST1/2 in mammals), the protein kinase complex LATS1/2-Mob1 phosphorylates several serine residues within the HXRXXS motif of YAP and when Ser^{127} is phosphorylated, YAP binds 14-3-3 proteins and is sequestered in the cytoplasm and subsequently degraded by the proteosome [19]. The angiomotin family members (AMOT, AMOTL1 and AMOTL2) also promote YAP inactivation by regulating YAP localization to the cytosol via their interactions with the actin cytoskeleton and YAP, leading to YAP phosphorylation by the Hippo cascade [20,21]. In the absence of Hippo or angiomotin negative regulation, YAP accumulates in the nucleus where it interacts mainly with the TEAD family of transcription factors to stimulate the expression of genes involved in growth, survival, mobility and invasion [22].

Significant evidence suggests crosstalk mechanisms exist between the mTOR and Hippo signaling cascades [23]. YAP has been demonstrated to regulate the mTOR pathway via effects on miR-29 expression [24]. Activation of YAP induced the transcription of miR-29 resulting in the inhibition of translation of PTEN, a critical negative regulator of PI3K. The blockade of PTEN by YAP activates PI3K signaling and leads to enhanced activity of mTORC1 and mTORC2. Additionally, G protein coupled receptors have been demonstrated to inhibit the Hippo pathway and activate YAP [25]. Thrombin, a ligand for the G-protein coupled receptor PAR1, activated YAP1 and inhibited PTEN expression [26]. In the context of TSC1 (hamartin) loss, mTOR has been shown to regulate YAP turnover in an ATG7-dependent manner. mTORC2 has also been shown to phosphorylate AMOTL2 at serine 760 resulting in the inability of AMOTL2 to bind and repress YAP leading to enhanced expression of YAP target genes [27].

In this report we present evidence that mTORC2 is able to directly phosphorylate serine 436 on YAP resulting in the enhancement of YAP activity. We demonstrate that modulation of mTORC2 activity coordinately regulates YAP transcriptional activity and YAP-dependent target gene expression. mTORC2 interacts with YAP via SIN1 and mutational analysis of serine 436 demonstrates that this phosphorylation event affects YAP stability, nuclear localization and TEAD association leading to enhanced transactivation. Moreover, cells expressing YAP serine 436 mutants display altered glioblastoma growth, migratory capacity and invasiveness both *in vitro* and in murine xenograft experiments. We further demonstrate that mTORC2 maintains its ability to regulate a Hippo pathway resistant allele of YAP suggesting that mTORC2 can regulate YAP independent of Hippo signaling. Correlative associations between the expression of these components in patient samples support the presence of this signaling cascade in GBM.

Materials and methods

Cell lines, GBM samples, Transfections and viral transductions

All GBM cell lines were obtained from ATCC except U87/EGFR and U87/EGFRvIII, which were kindly provided by Dr. Paul Mischel (Department of Pathology, Stanford University). The PDX lines GBM6 and GBM43 were kindly provided by Dr. Jann Sarkaria (PDX National Resource, Translational Neuro-Oncology, Mayo Clinic). Parental and $Sin1^{-/-}$ null MEFs were kindly provided by Dr. Bing Su (Department of Immunology and Microbiology, Shanghai Institute of Immunology). The LN229, T98G, and U87 GBM lines stably expressing either non-targeting control or Rictor targeting shRNAs have been previously described [7]. Lines were routinely tested to confirm the absence of mycoplasma and authenticated by STR profiling (ATCC). Flash-frozen normal brain and glioblastoma samples were obtained from the Cooperative Human Tissue Network under an approved Institutional Review Board protocol and informed consent obtained from each individual. Each sample was histopathologically reviewed and those containing greater than 95% tumor were utilized. Samples were homogenized in RIPA buffer using a Polytron homogenizer (Thomas Scientific, Swedesboro, NJ) followed by sonication to generate extracts for protein and RNA analysis. DNA transfections were performed using Effectene transfection reagent according to the manufacturer (Qiagen, Germantown, MD). For siRNA knockdowns, U87, GBM6 or GBM43 cells were transfected with 10 nmol/L siRNA pools targeting Rictor, Sin1 or a non-targeting scrambled control sequence. ON-TARGETplus siRNAs were obtained from Horizon Discovery Biosciences and transfected using Lipofectamine RNAimax (ThermoFisher Scientific). Lentiviral shRNA production and infection was performed as described [7].

Constructs and reagents

The YAP-5SA construct was obtained from Dr. Kun-Liang Guan (Department of Pharmacology, UCSD). The myc-tagged Rictor construct in pRK5 was obtained from Dr. David Sabatini (Whitehead Institute, MIT) and the EGFRvIII construct in pCMV6 was subcloned from PT3.5/CMV-EGFRvIII obtained from Dr. John Ohlfest (Department of Pediatrics, University of Minnesota). The Sin1Δ193-522 construct was generated by subcloning the appropriate sequences from pcDNA-mSin1(1.1)-HA obtained from Drs. Jie Chen and Taekjip Ha (University of Illinois at Urbana-Champaign) into pCMV6. The YAP-TEAD activity reporter HOP-flash and mutant TEAD binding site version was a gift from Dr. Barry Gumbiner (University of Virginia Health Sciences Center). Human YAP1, YAP-5SA or AKT1 were cloned into pT7-FLAG-1 for bacterial expression and purification of recombinant proteins. Mutagenesis was performed using the QuikChange Lightning Multi Site-Directed Mutagenesis Kit (Agilent Technologies) with the appropriate mutagenic primers to generate recombinant YAP1 S436 mutant alleles. The Flag-tagged native YAP1 and mutant alleles were subsequently subcloned into pCMV6 for mammalian expression. A TRC pLKO.1 library construct expressing shRNA-targeting the YAP1 3′ UTR (TRC designation TRCN0000107265) or non-targeting controls were also from Horizon Discovery Biosciences. DNA constructs composed of portions of SIN1 and YAP1 were generated by PCR and individually subcloned into the yeast two-hybrid plasmids pGB12 and pACT2, respectively. Yeast two-hybrid screening was performed using standard procedures [28]. Liquid β-gal assays were performed as previously described [7]. JR-AB2-011 was synthesized by Dr. Michael Van Zandt (New England Discovery Partners, Branford, CT). MK-2206 was from Selleckchem (Houston, TX). All other reagents were from Sigma-Aldrich.

Quantitative real time PCR

For quantitative RT-PCR, extraction of RNA was performed using Trizol (ThermoFisher Scientific). Total RNA was then quantified and integrity assessed using an Agilent 2100 Bioanalyzer (Agilent Technology). Total RNA was reverse transcribed with random primers using the RETROscript™ kit from Invitrogen. SYBR Green quantitative PCR (MilliporeSigma) was performed in triplicate in 96-well optical plates on an ABI Prism 7000 Sequence Detection System (ThermoFisher Scientific) according to the manufacturer's instructions. Primer sequences for CTGF and Cyr61 are available upon request.

Protein analysis, co-immunoprecipitations, in vitro kinase assays and YAP-TEAD reporter activity

Western blotting and Rictor-mTOR co-immunoprecipitations were performed as previously described [7] utilizing 0.3% CHAPS-buffer to maintain mTORC2 complex integrity during lysis in the course of immunoprecipitation. These precipitates were subsequently utilized in *in vitro* kinase assays as described [7]. Mnk1 and Raptor-mTOR were immunoprecipitated for kinase assays as previously described [29,30]. Antibodies to the following proteins were used: phospho-S^{473}-AKT (#9271, CST), phospho-S^{127}-YAP (#ab76252, Abcam), AKT (#9272, CST), Rictor (#A300-459A, Bethyl Laboratories), Raptor (A300-553A, Bethyl Laboratories), actin (#ab3280, Abcam), YAP1 (#12395S, CST), α-Flag (#TA50011, Origene), TEAD1 (#12292S, CST), TEAD2 (#ab92279, Abcam), TEAD3 (#13224S, CST), TEAD4 (#ab137833, Abcam), SMAD1 (#9743S, CST), p73 (#14620S, CST), FOS (#4384S, CST), TBX5 (#ab137833, Abcam), Mnk1 (#sc-133107, Santa Cruz Biotechnology), CTGF (#HPA031075, Sigma), Cyr61 (#NB100-356SS, Novus), Hsp90 (#SMC149B, StressMarq Biosciences), Lamin B2 (#12255S, CST) and mSin1 (#07-2276, MilliporeSigma). Anti-phospho- (Ser^{436})-hYAP1 antibody was generated in rabbits immunized with the phosphorylated peptide NQSTLP-pSQQNRF (where pS represents phosphoserine) and subsequently affinity purified. YAP-TEAD reporter activity was determined as previously described [31]. The HOP-flash (CTGF-luc) reporter contains multiple copies of *wt* TEAD-binding sites with a minimal CTGF promoter upstream of a luciferase reporter gene. The HIP-flash negative control reporter contains mutated TEAD binding sites (CTGFΔTB-luc). Luciferase activity was measured via a luciferase assay system (Promega).

Cellular fractionation and immunofluorescence

Nuclear-cytoplasmic fractionation was performed according to Dignam *et al.* [32]. Briefly, all buffers used were kept on ice and centrifugations were done at 4°C with soft braking. After a single wash with PBS, cells were scraped with PBS (containing 1 mM DTT and 1 × protease inhibitor) and harvested by centrifugation at 1000 × *g* for 15 min. The cell pellet was gently resuspended with 5 times the volume of pellet with buffer A (10 mM HEPES, pH 7.9, 1.5 mM $MgCl_2$, 10 mM KCl, 0.5 mM DTT, and 1 × protease inhibitor) and incubated on ice for 15 min, followed by homogenization (Wheaton). Cell lysis was monitored by trypan blue staining. The cell lysate was spun at 1000 × *g* for 5 min to collect the pellet as the nuclear fraction and the supernatant as the cytoplasmic fraction. For immunofluorescence staining, cells were grown on coverslips and were fixed with 4% paraformaldehyde in PBS for 15 min at room temperature (or overnight at 4˚C) and washed three times for 5 min in 100 mM glycine containing PBS, followed by permeabilization with 0.1% Triton X-100 in PBS for 10 min. After blocking with 3% nonfat dry milk in PBS for 1 h, cells were incubated with primary antibody diluted in 1% BSA/PBS overnight at 4˚C. After washing with PBS, cells were incubated with Alexa Fluor 488– or 594–conjugated secondary antibodies (Invitrogen) for 1 h and washed with PBS. Cell nuclei were counterstained and mounted with a mounting medium with DAPI (Vectashield; Vector Laboratories). Immunofluorescence images were collected at room temperature on a Zeiss Axio Imager M2 microscope coupled to a cooled digital CCD camera (ORCA-R^2 C10600-10B-H; Hamamatsu Photonics).

Clonogenic, cell proliferation and migration assays

Clonogenic assays were done by plating a total of 1,000 cells per well in 24-well plates in a total volume of 400 µL using a 2-layered soft agar system as previously described [7]. Viable cell numbers were determined via manual counting of cells stained with trypan blue. Cell migration assays were performed using modified Boyden chambers (MilliporeSigma) as previously described [7]. For invasion assays through Matrigel, 2×10^4 cells were placed into the top well of Boyden chambers containing growth factor-reduced Matrigel extracellular basement membrane over a polyethylene terephthalate membrane (8-mm pores; ThermoFisher Scientific). Following 24 h culture, Matrigel was removed and invaded cells were stained, solubilized and absorbance determined at 590 nm.

Xenograft studies

All animal experiments were performed under an approved Institutional Animal Care and Use Committee protocol. Xenografts of the LN229 YAP1 knockdown cell lines expressing *wt* YAP, the nonphosphorylatable S436A YAP1 or phosphomimetic S436E YAP1 alleles were injected s.c. into the flanks of 4 to 6 week old female C.B.-17-scid (Taconic) mice as previously described [33]. Sample sizes were chosen based on similar well-characterized experiments to ensure adequate power to detect a pre-specified effect size. Mice were randomly assigned to groups and the investigator blinded to assignments until final tumor analyses. Tumors were measured every 3 to 4 days and tumor volumes calculated using the formula length x width x height x 0.5236. Tumors were harvested at autopsy, weighed and mRNA isolated for expression analyses.

Statistical analysis

Statistical analyses were performed using unpaired Student's *t* tests and one-way ANOVA with Tukey's post hoc test using Systat 13 (Systat Software, Chicago, IL). *P* values of less then 0.05 were considered significant. Significance in group comparisons was determined using a one-way analysis of variance and data generated showed normal distribution with similar variances, and analysis was completed assuming equal variances. To assess correlations of molecular markers in glioblastomas Spearman's rank correlation was used.

Results

mTORC2 activation enhances YAP transcriptional activity and target gene expression

While YAP appears to be activated in many cancers, including glioblastoma, the mechanisms by which this can occur are unclear. Our previous studies [27], as well as the work of others [34], have suggested YAP may be a direct effector of mTORC2. To begin to investigate whether this may be the case, we examined YAP activity following stimulation of mTORC2 activity via co-transfection of a constitutively active EGFRvIII allele or a Rictor construct in conjunction with a YAP-TEAD transcriptional reporter construct. We included a dominant negative Sin1 mutant which has been demonstrated to significantly inhibit mTORC2 activity as a negative control [35]. As shown in figure 1A both EGFRvIII and Rictor were able to

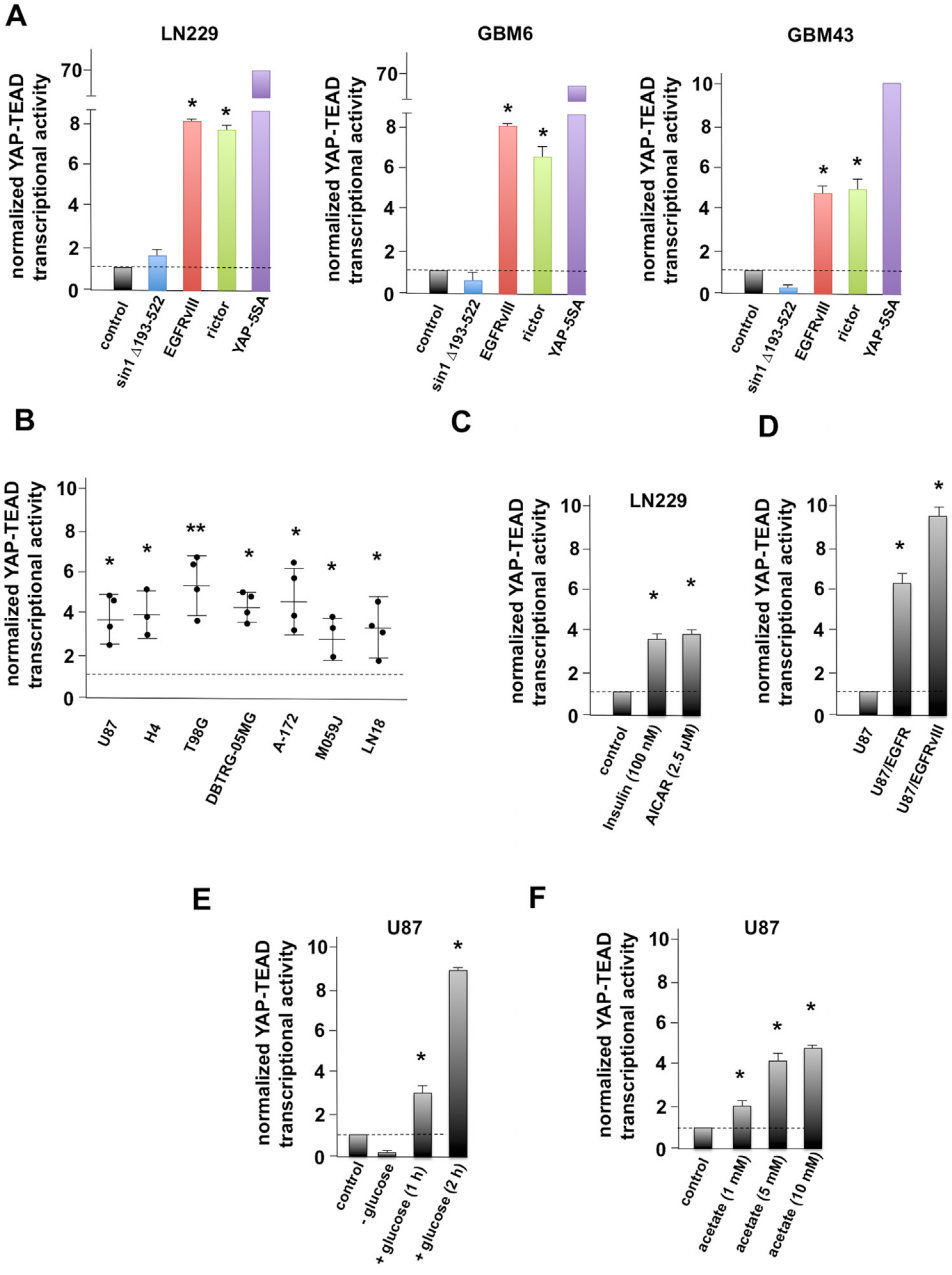

Fig. 1. mTORC2 promotes YAP activity and target gene expression in glioblastoma and PDX lines. (A) LN229, GBM6 and GBM43 cells were transiently transfected with the indicated constructs and YAP-TEAD luciferase reporter vector and following a 48 h incubation, reporter activity was assessed. Mean + S.D. are shown $n = 3$. * $P < 0.05$. (B) YAP-TEAD transcriptional activity was determined in the indicated GBM lines following transient transfection with either control or a Rictor expressing vector. Mean ± S.D. are shown, $n = 3$. * $P < 0.05$; ** $P < 0.01$. Scatter plots show mean ± S.D., where each dot is an independent experiment in which Rictor transfected cells were converted to fold increase over control cells indicated by the dotted line. (C) LN229 cells were transiently transfected with the YAP-TEAD luciferase reporter and subsequently treated with insulin (100 nM, 4 h) or AICAR (2.5 μM, 6 h) and reporter activity determined. Mean + S.D. are shown, $n = 3$. * $P < 0.05$. (D) Parental U87, U87 cells stably overexpressing native EGFR, and U87 cells stably overexpressing the constitutively active EGFRvIII variant [14], were transiently transfected with the YAP-TEAD luciferase reporter vector and reporter activity determined. Mean + S.D. are shown, $n = 3$. * $P < 0.05$. (E) YAP-TEAD luciferase reporter activity of U87 cells after 24 h of treatment with glucose deprivation (- glucose), combined with an add-back of glucose (+ glucose, 4.5 g/L) for the indicated time periods. Previous studies have demonstrated heightened mTORC2 activity following 2 h of glucose addition [37]. Mean + S.D. are shown, $n = 3$. * $P < 0.05$. (F) As in (E), however with the addition of acetate at the indicated concentrations for 12 h. Concentrations of acetate higher then 5 mM have previously demonstrated marked stimulation of mTORC2 activity [37]. Mean + S.D. are shown, $n = 3$. * $P < 0.05$.

increase YAP transcriptional activity in LN229 GBM cells and 2 PDX lines GBM6 and GBM43. The nonphosphorylatable mutant YAP5SA, which is not subject to Hippo pathway negative regulation, markedly stimulated YAP-TEAD reporter activity as expected. Moreover, overexpression of Rictor which has been demonstrated to increase mTORC2 activity [7], promoted YAP transcriptional activity in all GBM lines tested (Fig. 1B). Both insulin and the AMP kinase activator AICAR are known to stimulate mTORC2 activity [12,36], and treatment of LN229 cells with either significantly induced p-S^{437}-AKT expression (Supplemental Fig. S1A). Insulin and AICAR treatment also stimulated YAP-dependent reporter activity (Fig. 1C). In U87 cells stably transduced with either native EGFR or the constitutively active EGFRvIII allele, mTORC2 activity was increased (Supplemental Fig. S1B) as was YAP-TEAD transcriptional activity (Fig. 1D). Glucose or acetate has been demonstrated to promote mTORC2 signaling via acetyl-CoA production [37] (Supplemental Figs. S1 C&D) and we determined whether treatment of cells with either had affects on YAP-dependent transactivation. As shown in figures 1 E&F, exposure of U87 cells to glucose or acetate stimulated YAP-dependent reporter activity. These results demonstrate that elevated mTORC2 activity enhances YAP transcriptional activity in GBM cells.

Ablation of mTORC2 attenuates YAP transcriptional activity and target gene expression

We subsequently determined whether inhibition of mTORC2 activity would affect YAP transcriptional activity and target gene expression. We examined LN229, T98G and U87 GBM cells in which Rictor expression had been stably inhibited via shRNA-mediated knockdown. These lines had been previously demonstrated to harbor markedly reduced mTORC2 activity [7]. As shown in figure 2A inhibition of Rictor expression resulted in a significant inhibition of YAP transcriptional activity compared to cells expressing a non-targeting control shRNA. We also determined the affects of Rictor knockdown in the PDX lines GBM6 and GBM43 on YAP transcriptional activity. Rictor siRNA-mediated knockdown in these lines resulted in nearly undetectable levels of p-S^{473}-AKT (Supplemental Fig. S2A). Knockdown of Rictor in the PDX lines also resulted in significant inhibition of YAP transcriptional activity (Fig. 2B). Inhibition of Rictor expression furthermore resulted in downregulation of the YAP target genes *CTGF* and *Cyr61* in both established GBM lines (Fig. 2C) and in the PDX lines GBM6 and GBM43 (Fig. 2D). We tested the affects of pharmacological inhibition of mTORC2 activity using the mTORC2 specific inhibitor JR-AB2-011 [38] and determined whether YAP transcriptional activity and target gene expression was affected. As shown in figure 2E, treatment of a panel of GBM lines with JR-AB2-011 resulted in significant inhibition of YAP reporter activity as well as reductions in *CTGF* and *Cyr61* expression relative to control untreated cells (Figs. 2E&F). We also examined YAP transcriptional activity and target gene expression in $Sin1^{-/-}$ null MEFs. As shown in Supplemental figure S2B, $Sin1^{-/-}$ null MEFs displayed a significantly lower level of YAP reporter expression relative to *wt* MEFs and similarly expressed reduced *CTGF* and *Cyr61* mRNA levels. Taken together, these data show that inhibition of mTORC2 results in marked reductions in YAP activity and target gene expression in GBM cells.

mTORC2 targets YAP1 via Sin1-dependent interaction and phosphorylates serine 436

Our previous data have demonstrated that the angiomotin-like 2 protein is negatively regulated via phosphorylation at serine 760 by mTORC2 [27]. This phosphorylation event renders AMOTL2 unable to bind to YAP and represses its activity, leading to elevated nuclear associated YAP and activation of YAP-target genes. Thus, increased mTORC2 activity via effects on AMOTL2, coordinately regulates an increase in YAP function to promote GBM proliferation, mobility and invasiveness. However, our data also suggested that GBM cells harboring elevated mTORC2 activity might have direct effects on YAP. To investigate this, we performed large-scale yeast 2-hybrid screens using full-length human Sin1 as bait which was screened against libraries prepared from U87EGFRvIII or insulin-stimulated LN229 cells in which mTORC2 was hyperactive. We were able to identify most of the known Sin1 protein partners (Rictor, mTOR, PCBP2, SFN, CDC42EP1, ATF2, MAP3K2, MAPK8, IFNAR2 and SGK1) in these screens [39] (Supplemental fig. S3A). In addition to the known SIN1 partners, we also identified novel Sin1 interacting proteins. We identified YAP1 and mapped the interacting domains of the two proteins by generating a series of deletion mutants and assessed their ability to associate via the two-hybrid assay (Supplemental fig. S3B). This interaction was also confirmed by co-IP experiments of endogenous proteins in U87 GBM cells (fig. 3A). Reasoning that this interaction may serve as a basis for mTORC2-mediated phosphoregulation of YAP we ascertained whether YAP could be phosphorylated *in vitro* by activated mTORC2. As shown in figure 3B, YAP is efficiently phosphorylated in mTORC2 *in vitro* kinase assays in the presence of γ^{32}P-ATP and the indicated substrates. Additionally, mTORC2 was able to phosphorylate the LATS nonphosphorylatable YAP-5A mutant when utilized as a substrate in these reactions. Analysis of the YAP protein sequence identified a highly conserved consensus mTOR phosphorylation site, serine 436, within the transactivation domain of YAP (Supplemental figure S3C). Phosphospecific antibodies were generated against this site and utilized in mTORC2 *in vitro* kinase assays demonstrating mTORC2 phosphorylation of YAP at this residue while an alanine S436 substitution mutant and inclusion of the TORKI inhibitor PP242 in the *in vitro* kinase assays blocked YAP phosphorylation (fig. 3C). Insulin treatment led to increased phospho-S^{436} YAP levels (fig. 3D) while Rictor (fig. 3E) or Sin1 (fig. 3F) knockdown in U87 cells resulted in significantly reduced phospho-S^{436} YAP levels. As AKT has been previously demonstrated to phosphorylate YAP at serine 127 in response to DNA damage [40], we ascertained whether modulation of mTORC2 affected S^{127} phosphorylation. S^{127} YAP phosphorylation status was unaffected by insulin stimulation of mTORC2 or knockdown of Rictor or Sin1 (see figs. 3D-F). Moreover, pharmacological inhibition of Akt activity did not appear to affect phospho-S436 YAP levels in U87 cells (Supplemental figure S3D). Our interaction screens did not identify the YAP paralog TAZ as a Sin1 binding partner and sequence analysis of TAZ did not reveal a similarly conserved mTORC2 phosphorylation site within the TAD domain.

A phosphomimetic S436E YAP mutant is markedly stabilized, accumulates in the nucleus, promotes TEAD association and induces YAP transcriptional activity

To determine the functional affects of the serine 436 phosphorylation event on YAP we initially examined whether the YAP S^{436} nonphosphorylatable and phosphomimetic mutants exhibited altered protein stability in cycloheximide-chase assays. As shown in figure 4A, U87 cells stably expressing flag-tagged versions of native, S436A-YAP and S436E-YAP proteins were treated with cycloheximide and the half-lives of the mutant proteins determined. As shown, native YAP displayed a half-life of 1.7 h and the nonphosphorylatable S436A YAP mutant exhibited a comparable half-life of 1.9 h. However, the half-life of the phosphomimetic S436E YAP mutant was markedly increased to greater then 8 h. We subsequently examined whether the mutant YAP proteins displayed altered nucleocytoplasmic localization. Shown in figure 4B, in cell fractionation experiments, wild-type YAP displayed both cytoplasmic and nuclear abundances in U87 cells, however significantly more native YAP was found in the cytoplasmic fraction. The nonphosphorylatable S436A YAP mutant displayed significantly more cytoplasmic localization as compared to native YAP and the phosphomimetic S436E YAP mutant accumulated in nuclear fractions. We also assessed nuclear versus cytoplasmic localization

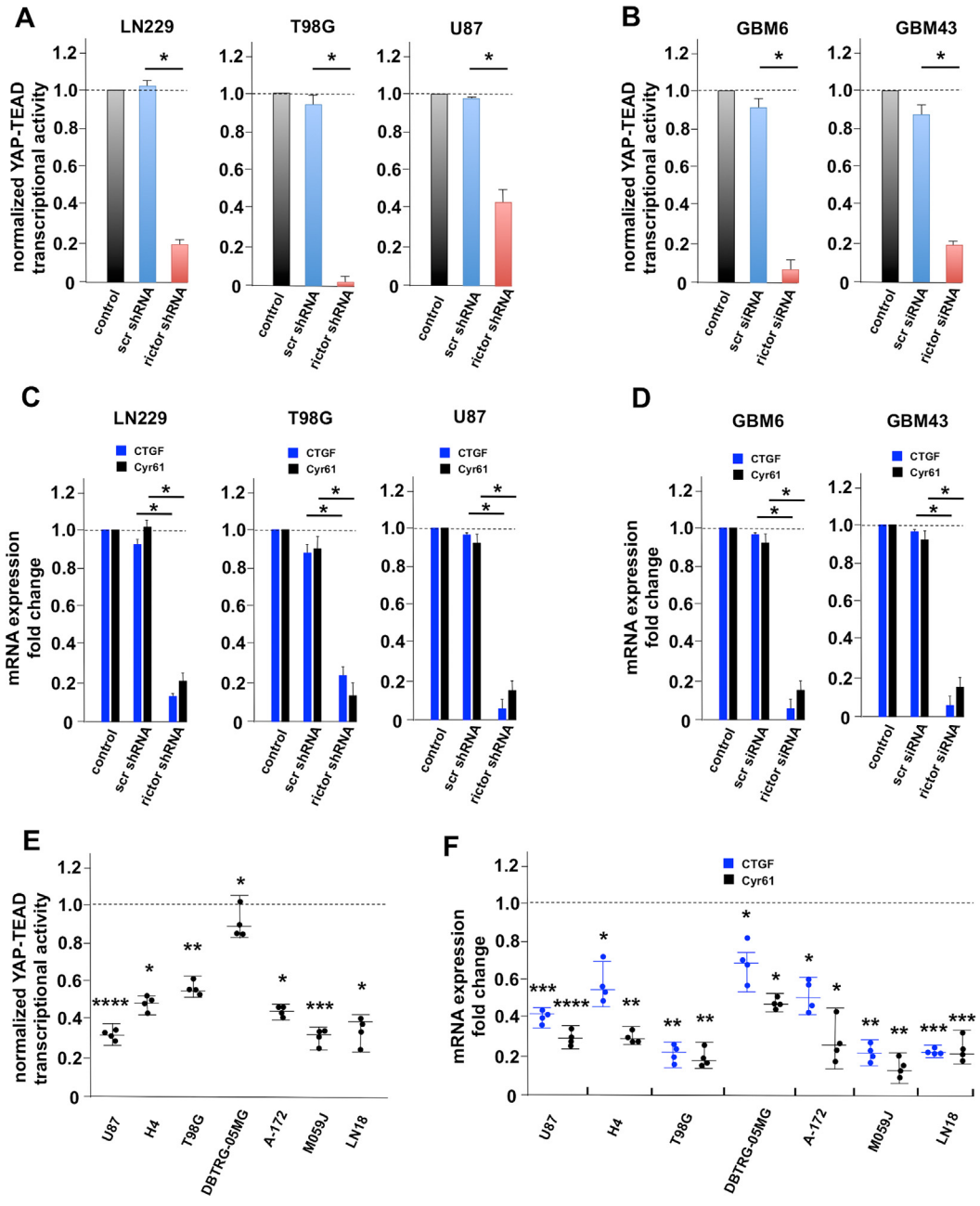

Fig. 2. mTORC2 inhibition suppresses YAP transcriptional activity and target gene expression. (A) YAP-TEAD luciferase reporter activity was determined for the indicated GBM lines stably expressing either a non-targeting scramble (scr) shRNA or a Rictor targeting shRNA. Mean + S.D. are shown, $n = 3$. * $P < 0.05$. (B) Inhibition of YAP-TEAD luciferase reporter activity in GBM6 and GBM43 PDX lines in which Rictor expression was blocked via siRNA-mediated knockdown as indicated. Mean + S.D. are shown, $n = 3$. * $P < 0.05$. (C) Expression of YAP-dependent target mRNAs *CTGF* and *Cyr61* in the indicated GBM lines following knockdown of Rictor via shRNA. mRNA was isolated and subjected to quantitative rt-PCR analyses. qRT-PCR measurements were performed in quadruplicate and the mean and + S.D. are shown. * $P < 0.05$. (D) Inhibition of *CTGF* and *Cyr61* mRNA expression in GBM6 and GBM43 following siRNA-mediated knockdown of Rictor expression as determined by qRT-PCR analyses. Mean + S.D. are shown. $n = 4$. (E) The indicated GBM lines were transiently transfected with the YAP-TEAD luciferase reporter and treated with JR-AB2-011 (1 μM, 8 h) and YAP-TEAD reporter activity determined relative to control untreated cells. Mean ± S.D. are shown, n = 3. * $P < 0.05$; ** $P < 0.01$; *** $P < 0.001$; **** $P < 0.0001$. (F) Inhibition of YAP-dependent *CTGF* and *Cyr61* mRNA expression in the indicated GBM lines in the presence of JR-AB2-011 (1 μM, 8 h) relative to untreated controls. qRT-PCR measurements were performed in quadruplicate and the mean and ± S.D. are shown. * $P < 0.05$; ** $P < 0.01$; *** $P < 0.001$; **** $P < 0.0001$.

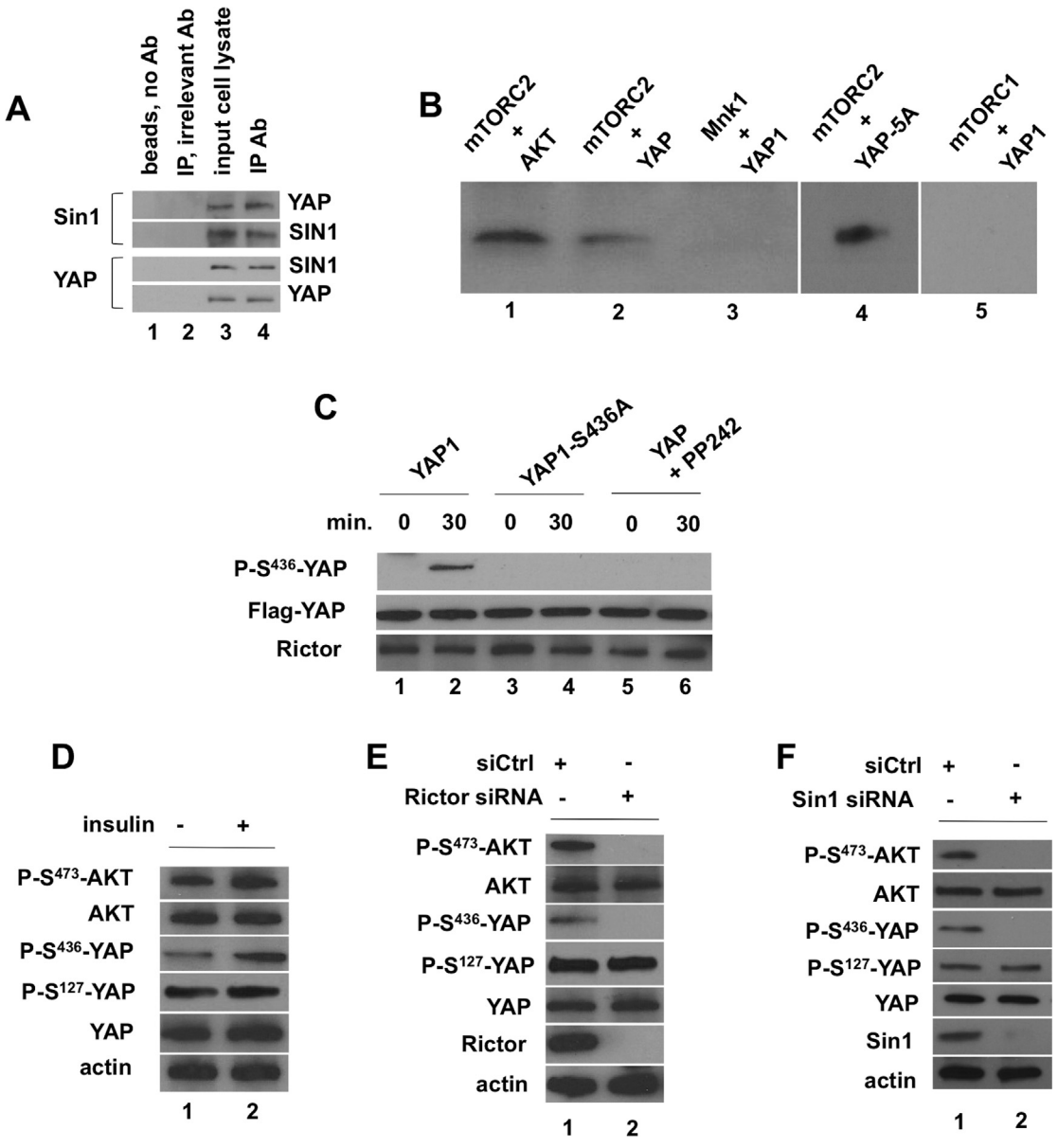

Fig. 3. YAP interacts with the mTORC2 component Sin1 and is phosphorylated on serine 436. (A) Co-immunoprecipitation of endogenous Sin1 and YAP. U87 cell extracts were immunoprecipitated with either Sin1 or YAP antibodies and immunoprecipitates subjected to immunoblot analysis for the indicated proteins. Lane 1, beads, no antibody; lane 2, immunoprecipitation with an irrelevant antibody (control IgG), lane 3, input cell lysate; lane 4 indicated immunoprecipitate probed with antibodies for the indicated proteins. (B) An *in vitro* kinase assay was performed with Rictor-immunoprecipitated mTORC2 from U87 cell lysates in the presence of recombinant AKT, native YAP or mutant YAP-5A as indicated in the presence of γ^{32}P-ATP. Reactions were separated by SDS-PAGE followed by autoradiography. As negative controls, immunoprecipitated Mnk1 kinase or Raptor-immunoprecipitated mTORC1 was also used in the presence of YAP1, neither of which displayed detectable phosphorylation. (C) An mTORC2 *in vitro* kinase assay was performed utilizing Rictor immunoprecipitates isolated from U87 cells and incubated with purified native or S436A mutated recombinant Flag-tagged YAP for the indicated time points. Reactions containing native YAP were performed in the absence or presence of PP242 as shown. Kinase reactions were subsequently immunoblotted using a phospho-specific antibody generated against phospho-Ser^{436}-YAP, Flag or Rictor antibodies for detection. (D) Effects of insulin stimulation in U87 cells. Cells were stimulated with insulin (10 nM, 5 h), lysed and extracts immunoblotted for the indicated proteins. (E) U87 cells were treated with siRNAs targeting Rictor or non-targeting control (siCtrl) for 24 h and cell lysates analyzed by immunoblotting for the indicated proteins. (F) As in (E) except U87 cells were treated with siRNAs targeting Sin1 or non-targeting control (siCtrl).

of the mutant YAP alleles via immunofluorescence experiments (fig. 4C). Consistent with the cell fractionation experiments, native YAP was found localized to both the nucleus and cytoplasm and the nonphosphorylatable S436A YAP mutant was enriched in cytoplasmic fractions, while the phosphomimetic S436E YAP mutant was found redistributed to the nuclear compartment. Moreover, we determined whether in U87 cells expressing the native, nonphosphorylatable S436A, or phosphomimetic S436E YAP mutants demonstrated binding to TEAD family members (TEADs 1−4) or other transcription factors reported to interact with YAP (SMAD1, p73, FOS and TBX5). As determined via co-immunoprecipitation assays, TEADs 1−4

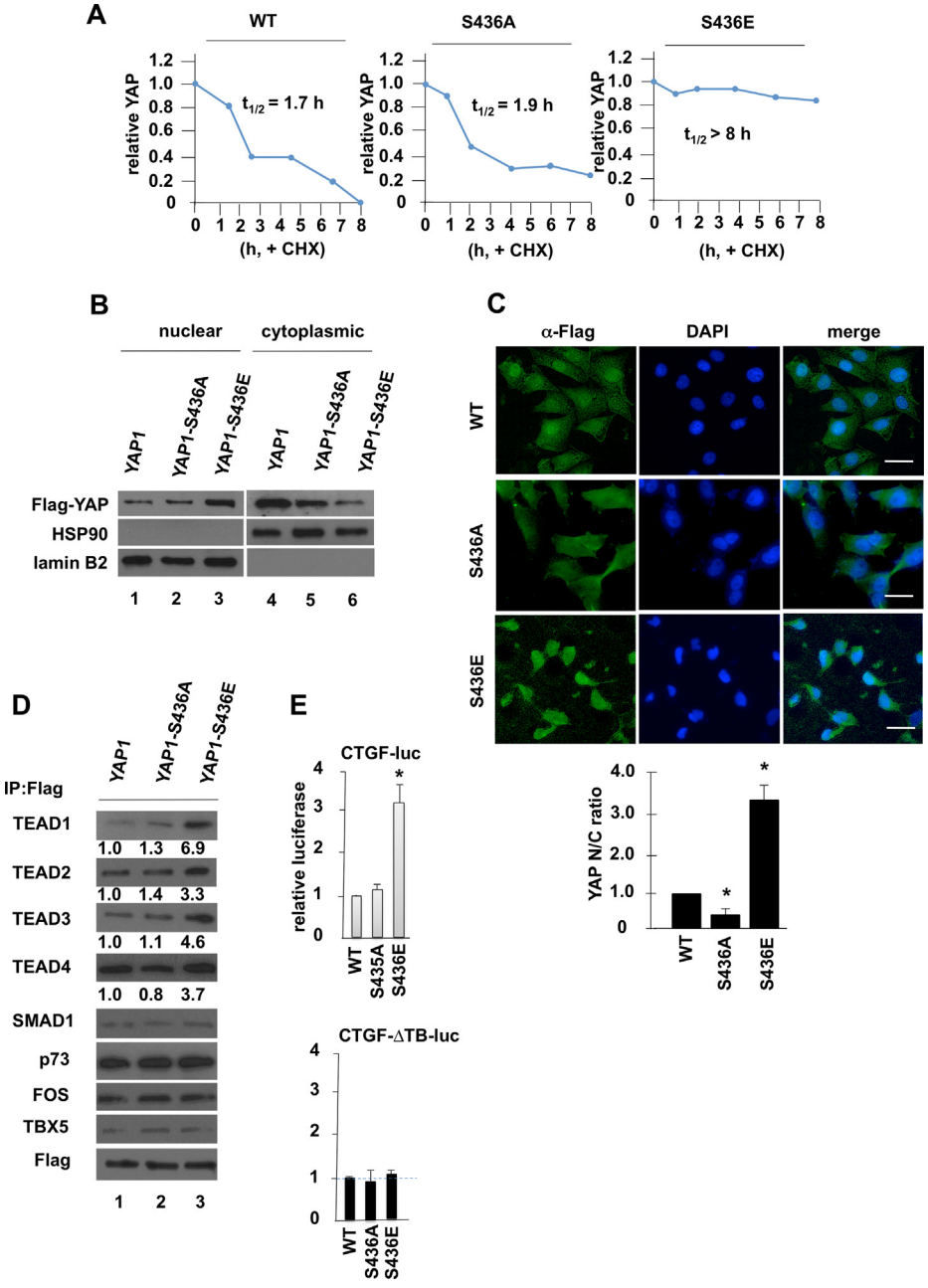

Fig. 4. A phosphomimetic S436E YAP mutant is stabilized, accumulates in the nucleus, promotes TEAD association and induces YAP target gene expression. (A) Mutation of S436 to alanine stabilizes YAP. U87 cells were transfected with the indicated Flag-tagged YAP constructs and treated with 50 μg/ml of CHX for the indicated time points. Transfected YAP levels were determined by α-Flag immunoblot. Relative YAP levels were quantified using the ratio between Flag-YAP and actin, which was set to 1 at the 0 time point. (B) Nuclear and cytoplasmic accumulation of native YAP, nonphosphorylatable S436A YAP and phosphomimetic S436E YAP mutant alleles. Nuclear and cytoplasmic fractions from U87 cells stably expressing the indicated Flag-tagged YAP alleles were immunoblotted using α-Flag, HSP90 or lamin B2 antibodies as shown. (C) Indirect immunofluorescence analysis of YAP S436 mutant localization in U87 cells expressing the indicated mutants. Shown below the representative images is the quantification of the nuclear/cytoplasmic ratio (N/C ratio) of YAP in U87 cells expressing the indicated YAP S^{436} mutants. Mean and + S.D. are shown. * $P < 0.05$. Cells were grown on coverslips, permeabilized, and stained with α-Flag antibodies and FITC-conjugated secondary. Nuclei were stained with DAPI. Scale bar, 20 μm. (D) The indicated Flag-tagged YAP1 alleles were expressed in U87 cells and immunoprecipitated with α-Flag antibodies. Expression values are shown beneath the TEAD1-4 blots which displayed significantly increased binding to YAP1-S436E. Immunoprecipitates were blotted for the indicated proteins. (E) Luciferase activity of U87 cells expressing the indicated YAP mutants and containing the CTFG-luc (*upper panel*) or CTFG-ΔTB1-3-luc (*lower panel*) promoter reporters.

bound the S436E YAP mutant to a greater degree as compared to SMAD1, p73, FOS and TBX5 (fig. 4D). The phosphomimetic S436E YAP mutant also markedly induced expression of a CTGF promoter-based luciferase reporter as compared to cells expressing native or the nonphosphorylatable S436A mutant (fig. 4E, *upper panel*). As a negative control we additionally tested a mutant version of the YAP responsive CTGF-luciferase reporter in which all three TEAD binding sites had been mutated. Experiments utilizing this reporter did not demonstrate reporter induction in cells expressing the phosphomimetic S436E mutant (fig. 4E, *lower panel*). These data demonstrate that the S436 YAP phosphorylation event promotes YAP stabilization, increases nuclear localization and association with TEAD family members, and promotes YAP-dependent transcriptional activity consistent with the activation of YAP by mTORC2-mediated phosphorylation.

YAP ser^{436} mutants affect growth, migratory capacity and invasiveness in GBM

We then examined whether the serine 436 phosphorylation event had effects on YAP-mediated cellular functions. To examine whether the S^{436} YAP1 phosphorylation event may promote glioblastoma characteristics we examined LN229 GBM cells in which the endogenous protein was abrogated via RNAi-mediated targeting. This was accomplished by stable expression of an shRNA targeting the 3′ UTR of YAP1 (Supplemental fig. S3E). These cells were subsequently stably transfected with vectors expressing native YAP, nonphosphorylatable S436A YAP or phosphomimetic S436E YAP alleles. We initially determined whether expression of the YAP serine 436 mutants would have affects on anchorage-independent growth relative to native YAP in soft agar assays. LN229$_{shYAP1}$ cells stably expressing wild-type YAP, S436A YAP, or S436E YAP were suspended in soft agar and the numbers of foci determined following 14 days of incubation. As shown in figure 5A, native YAP induced foci formation and expression of the nonphosphorylatable S436A YAP mutant reduced these numbers, however expression of the phosphomimetic S436E YAP mutant markedly increased foci numbers relative to values observed in cells expressing native YAP. As shown in figure 5B, cell proliferation was significantly induced by native YAP, however the nonphosphorylatable S436A YAP mutant displayed reduced cell numbers, while the phosphomimetic S436E YAP mutant markedly stimulated cell proliferation. YAP-induced migratory capacity (fig. 5C) was also significantly inhibited in cells expressing the nonphosphorylatable S436A YAP mutant and impeded the ability of cells to migrate towards either vitronectin or fibronectin coated transwell chambers as compared to cells expressing native YAP. However, cells expressing the phosphomimetic S436E YAP mutant were much more motile relative to cells expressing native YAP. Similarly, the ability of cells expressing the nonphosphorylatable S436A YAP mutant to invade Matrigel coated chambers was markedly reduced relative to cells expressing native YAP, while cells expressing the phosphomimetic S436E YAP mutant were significantly more invasive compared with cells expressing native YAP (fig. 5D).

mTORC2 is able to regulate YAP activity independent of Hippo pathway signaling

As Hippo pathway signaling appears to be attenuated in a significant number glioblastoma owing to promoter hypermethylation and/or miRNA-mediated inhibition of the LATS1/2 serine/threonine kinases [41], which are direct negative regulators of YAP, we were interested if mTORC2 could regulate YAP activity in the absence of Hippo signaling. We initially determined whether pharmacological inhibition of mTORC2 would result in reduced ser^{436} YAP levels and as shown in figure 6A, treatment with the mTORC2 inhibitor resulted in marked inhibition of ser^{436} phosphorylated YAP in LN229 cells and two GBM PDX lines, GBM6 and GBM43. We subsequently utilized the knockdown shRNA YAP1 LN229 cells in which endogenous YAP had been abrogated and transfected these cells with either native YAP or the constitutively active nonphosphorylatable YAP-5SA mutant and treated these cells with either the mTORC2 inhibitor or insulin to modulate mTORC2 activity. As shown in figure 6B, in cells in which native YAP expression was rescued, YAP-dependent target gene expression was inhibited by JR-AB2-011, while insulin markedly stimulated YAP-target gene expression. Similarly, in cells expressing the YAP-5SA mutant, resistant to inhibition by LATS phosphorylation, JR-AB2-011 inhibited YAP-dependent target gene expression, while insulin exposure induced YAP-target gene expression (fig. 6C). These data suggest that mTORC2 is able to regulate YAP via ser^{436} phosphorylation irrespective of Hippo pathway status.

The S436 YAP mutants alter growth of GBM xenografts

To determine whether the phosphomimetic S436E YAP mutant would alter the growth rate of GBM cells *in vivo*, we subcutaneously implanted LN229 shRNA YAP1 knockdown cells stably expressing the constructs indicated in figure 7A in SCID mice and monitored growth. Cells in which YAP expression had been blunted (LN229$_{shYAP1}$) displayed reduced growth with a latency period of 28 days as compared to the control non-targeting (scramble sequence) line (LN229$_{sh\ scr}$; latency period 14 days) or LN229$_{shYAP1}$/wt-YAP1 cells in which native YAP had been reintroduced (latency period 14 days). We also examined cells expressing either the nonphosphorylatable S436A YAP or the phosphomimetic S436E YAP mutants and as shown, the nonphosphorylatable S436A YAP mutant cells grew significantly slower relative to control or YAP rescued cells (latency period 31 days), while the phosphomimetic S436E YAP expressing cells displayed markedly increased growth (latency period 9 days). Overall survival of mice harboring the nonphosphorylatable S436A mutant cells was significantly longer then control or YAP rescued tumors and mice implanted with the phosphomimetic S436E YAP expressing cells had reduced survival (fig. 7B). Tumors from mice at autopsy were weighed and as shown in figure 7C, tumor weights reflected the observed differences in *in vivo* growth. Moreover, as shown in figure 7D, YAP-dependent target gene expression was similarly inhibited in the nonphosphorylatable S436A YAP mutant expressing cells and significantly induced in the phosphomimetic S436E YAP mutant line. These data support the results obtained *in vitro* (fig. 5) and suggest the mTORC2-mediated phosphorylation of ser^{436} regulates YAP-dependent growth of tumors in mice.

mTORC2/YAP signaling in GBM patients

To determine whether this signaling relationship was valid in clinical samples we examined an independent set of 27 flash-frozen GBM and 6 normal brain samples. Tumors were confirmed histologically, cell extracts prepared, and the total relative abundance of phospho- S^{473}-AKT, phospho-S^{436}-YAP1, YAP1, CTGF and Cyr61 determined by Western analyses. These data are summarized in Table 1 and supplemental figure S4. As shown, elevated mTORC2 activity, ascertained by immunoblotting for phospho-S^{473}-AKT levels was found in 17 of 27 tumor samples (63%, $P < 0.05$) consistent with numbers of GBM tumors harboring hyperactive mTORC2 from previous studies [7,14]. Phospho-S^{436}-YAP1 expression, YAP1, CTGF and Cyr61 expression was elevated in 63% (17 of 27, $P < 0.05$), 59% (16 of 27, $P < 0.05$), 78% (21 of 27, $P < 0.05$) and 70% (19 of 27, $P < 0.05$) of samples, respectively. Significant direct correlations were observed between samples containing elevated phospho-S^{473}-AKT and increased phospho-S^{436}-YAP, YAP1, CTGF and Cyr61. We also observed significant direct correlations between samples harboring elevated phospho-S^{436}-YAP1 expression and elevated YAP1 and increased CTGF or Cyr61 expression consistent with our previous *in vitro* data demonstrating the effects

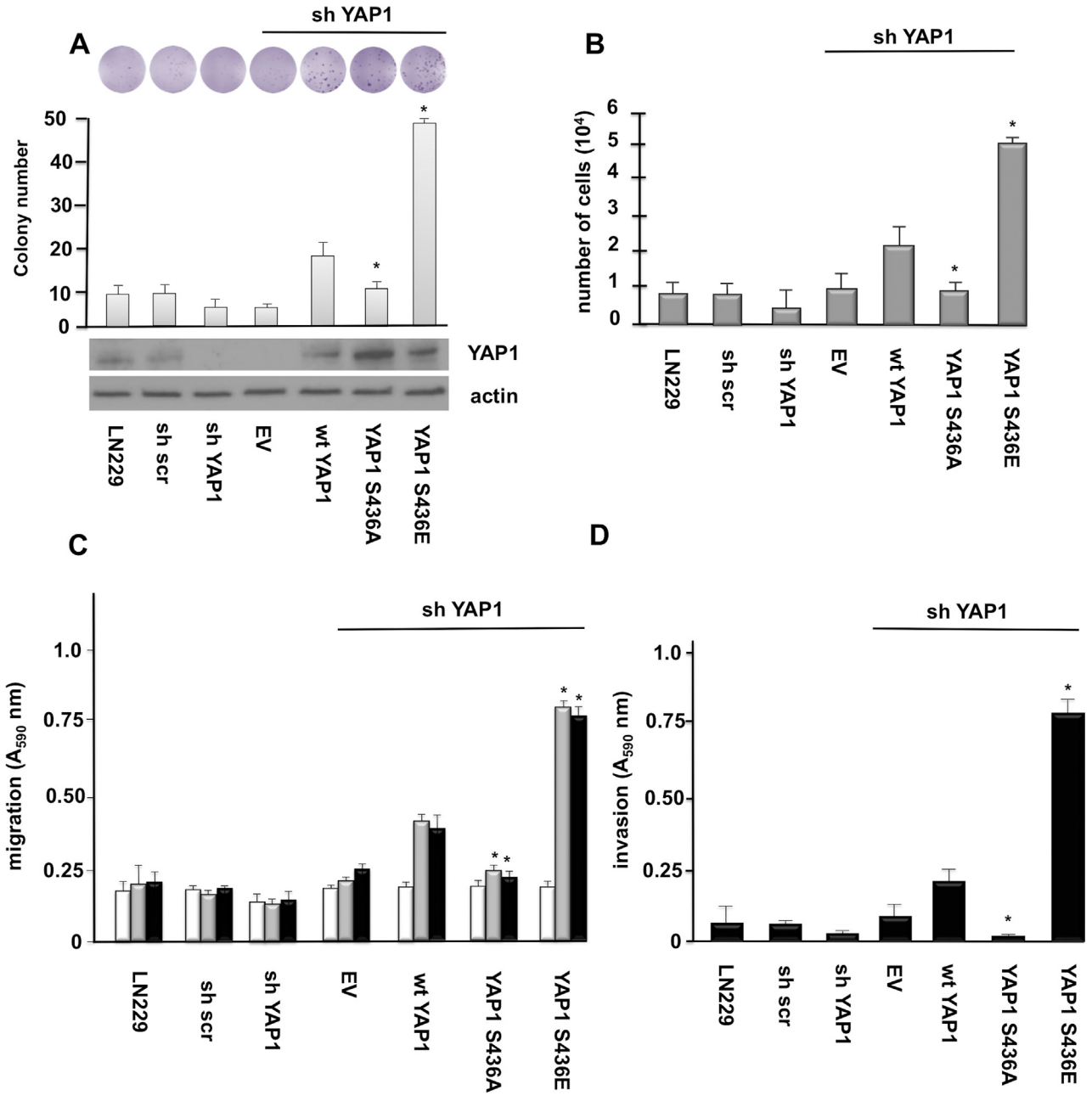

Fig. 5. YAP S436 mutants display altered GBM properties *in vitro.* (A) Effects of YAP S436 mutation on colony formation in $LN229_{shYAP1}$ cells in soft agar colony formation assays. $LN229_{shYAP1}$ cells were stably transfected with the indicated vectors (EV, empty vector control) expressing *wt* YAP1, YAP1 S436A, or YAP S436E alleles. 1,000 cells were suspended in soft agar and following 14 days of incubation colonies were stained and counted under an inverted microscope. Mean + S.D., n = 3. YAP1 allele expression of the indicated lines as shown in the immunoblot analyses probed for YAP1 and actin below the graph. Representative crystal violet stained images are shown above the graph. (B) The indicated lines expressing native, S436A YAP1, or S436E YAP1 alleles were seeded at 5×10^3 cells/well and cultured for 48 h and viable cell numbers determined by trypan blue exclusion. Mean and + S.D. are shown. * $P < 0.05$, n = 3. (C) Migration of the indicated cell lines expressing *wt* YAP1, YAP1 S436A, or YAP1 S436E alleles. Cells were seeded transwell chambers and allowed to migrate towards BSA (white bars), vitronectin (gray bars) or fibronectin (black bars). * $P < 0.05$. Data represent mean + S.D. of three independent experiments. (D) Invasive potential of the indicated lines expressing *wt* YAP1, YAP1 S436A, or YAP1 S436E alleles migrating through Matrigel. Data represent mean +S.D. of three independent experiments.

of this phosphorylation event on YAP stability, nuclear localization and TEAD association (see figs. 4A-C) ($P < 0.05$ for all correlations). These data support the signaling between mTORC2 and YAP1 observed in our cell line experiments and provide strong evidence for this signaling relationship in GBM patient samples.

Discussion

Hippo and mTOR signaling have emerged as two critical cascades coordinately regulating cell growth and division and thus, major nodes of interaction are anticipated to exist between these pathways [42]. Our previous

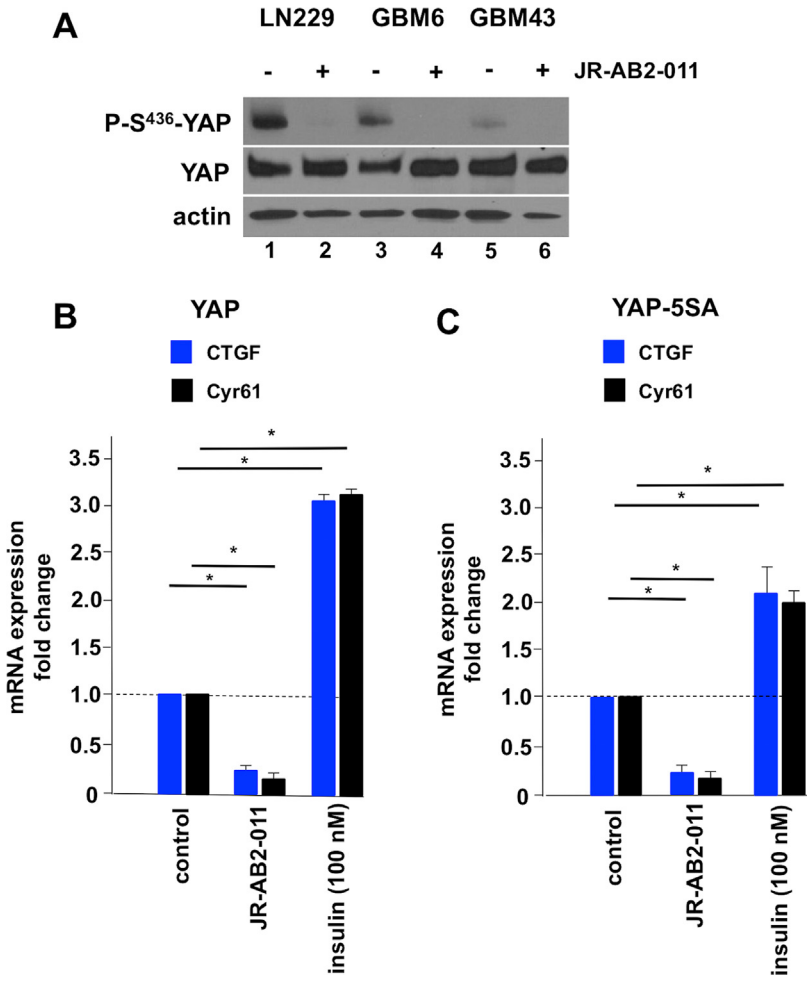

Fig. 6. mTORC2-mediated YAP S436 phosphorylation can occur independent of Hippo pathway signaling in GBM. (A) Inhibition of YAP S436 phosphorylation by JR-AB2-011 (1 μM, 8 h) in the indicated lines. Immunoblots were probed for phospho-S436 YAP, total YAP and actin as shown. (B) *CTGF* and *Cyr61* mRNA expression in $LN229_{shYAP1}$ cells expressing native YAP or LATS-resistant YAP-5SA mutant (C) following treatment with either JR-AB2-011 (1 μM, 8 h) or insulin (100 nM, 4 h) relative to control untreated cells. mRNA was isolated and subjected to qRT-PCR analyses. qRT-PCR measurements were performed in quadruplicate and the mean and + S.D. are shown. * $P < 0.05$.

data suggested a mechanism by which the mTORC2 signaling axis indirectly regulated YAP activity via affects on AMOTL2 [27]. In an extension of this work, we provide evidence that mTORC2 is also able to directly affect YAP function. Our work supports a model wherein mTORC2 is able to directly phosphorylate ser^{436} of YAP1 and stimulate YAP resulting in the elevated expression of YAP target genes (see fig. 7E).

Our data suggests that residues 1-136 of Sin1, which are conserved among all Sin orthologs except Sin1.4, is critical for recruitment of YAP to mTORC2 (Supplemental figure S3B). This region of Sin1 has unknown function and is directly N-terminal to the CRIM domain which is responsible for recruitment of AKT to mTORC2 [35,39]. We hypothesize that these residues may constitute a domain which recruits YAP to mTORC2 in an analogous manner to the CRIM domain. Residues 160−275 of YAP contain tandem WW domains mediating protein-protein interactions. We noted that within residues 1-136 of Sin1 is a proline rich motif which the WW domains of YAP may recognize. The Sin1-YAP interaction may serve a scaffolding function promoting mTORC2 phosphorylation of YAP.

It has been previously reported that YAP ser127 is phosphorylated by AKT [40]. As AKT is a major downstream effector of mTORC2 we examined whether modulation of mTORC2 activity would affect YAP ser127 phosphorylation. We did not observe alterations in YAP S127 phosphorylation upon insulin stimulation, Rictor or Sin1 knockdown (fig. 3D-E). This is consistent with studies from the Guan laboratory which also found that phosphorylation of YAP S127 was not affected in PDK1 knockout cells (in which AKT is quiescent) or by EGF, insulin, PI3K inhibitors or AKT overexpression [43]. Moreover, the nonphosphorylatable LATS YAP-5A mutant could be phosphorylated by mTORC2 (fig. 3B) and treatment of cells with the AKT inhibitor MK-2206 did not appear affect YAP S436 phosphorylation levels (supplemental fig. S3D). These data support the direct phosphorylation of YAP via mTORC2 and further suggest that AKT mediated phosphorylation of YAP is not subject to regulation via mTORC2 under these conditions. The lack of observed regulation in our experiments may reflect differences in cellular states, in that the reported AKT mediated phosphorylation of YAP occurs in response to DNA damage and thus AKT may become activated by mTORC2-independent mechanisms in those settings.

The observation that the phosphomimetic S436E mutant YAP exhibits increased stability, nuclear localization, TEAD-binding and transactivation capacity suggests that mTORC2 mediated mono-phosphorylation of this residue influences YAP through multiple mechanisms. Consistent with this, SRC and other SRC family kinases have been shown to directly phosphorylate YAP or TAZ (Y357) to promote their protein stability,

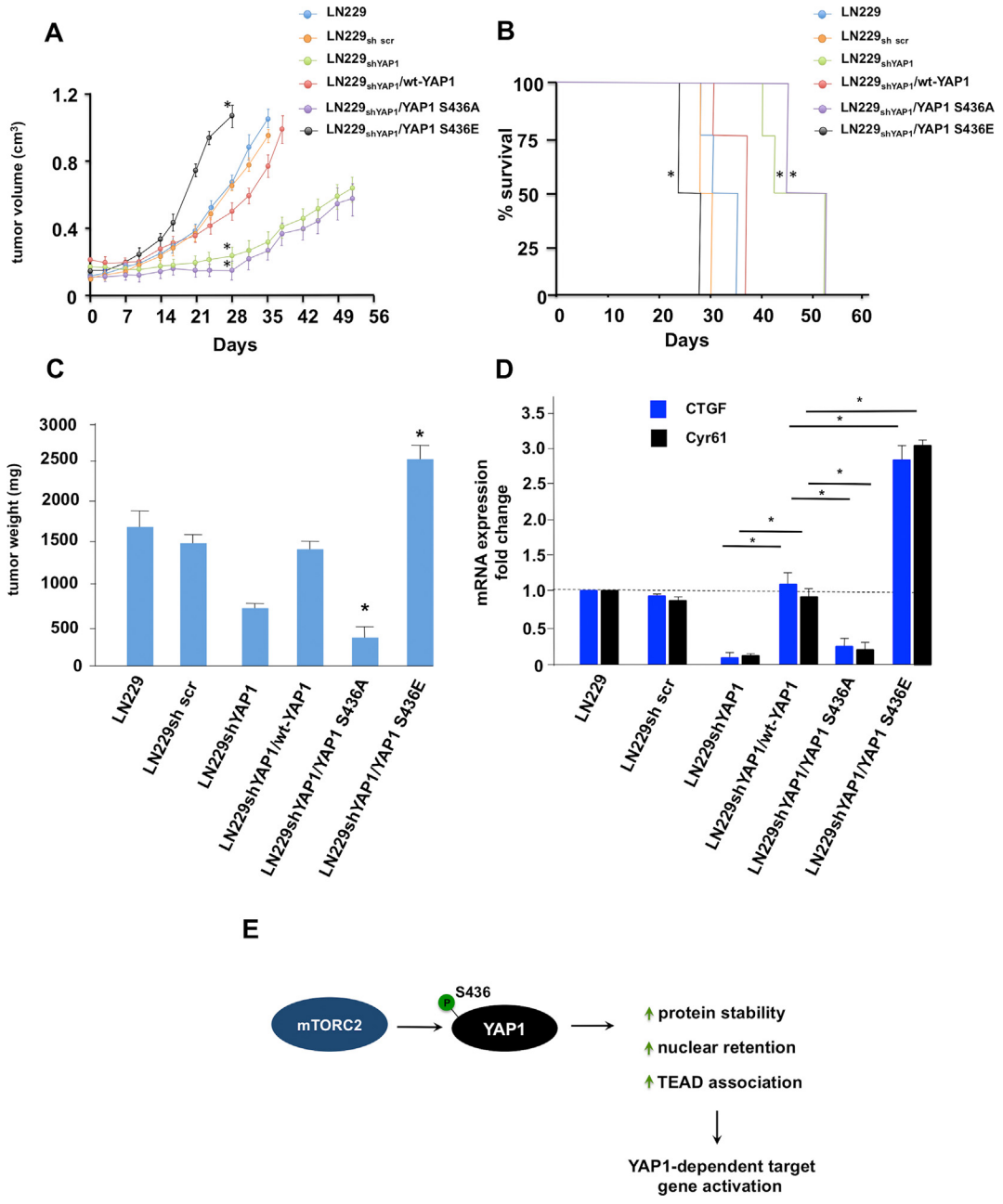

Fig. 7. Growth of YAP S436 mutant expressing GBM cells *in vivo*. (A) LN229$_{shYAP1}$ cells stably expressing native YAP1, nonphosphorylatable YAP1 S436A, or the phosphomimetic YAP1 S436E alleles were monitored for tumor growth for up to 52 days following establishment of ~200 cm^3 subcutaneous tumors in SCID mice ($n = 4$-5 per group). (B) Overall survival of mice with harboring the indicated S436 YAP mutant subcutaneous implanted LN229 tumors. *, $P < 0.05$, n = 4-5 mice per group. (C) Weight of tumors harvested at autopsy from xenografted mice implanted with the indicated GBM cells. * $P < 0.05$. (D) *CTGF* and *Cyr61* mRNA expression from harvested tumors cells expressing the indicated YAP1 alleles. mRNA was isolated and subjected to qRT-PCR analyses. qRT-PCR measurements were performed in quadruplicate and the mean and + S.D. are shown. * $P < 0.05$. (E) mTORC2 mediated phosphorylation of serine 436 of YAP1 leads to increases in protein stability, nuclear localization and TEAD association resulting in enhancement of YAP1 target gene expression.

transcriptional activity, and/or interaction with other transcription factors [44,45]. MK5 has also been shown to positively regulate YAP stability and YAP-TEAD transcriptional activity [46]. Both MK5 and SRC have been shown to influence YAP through distinct Hippo pathway signaling-independent mechanisms [44,46]. mTORC2 was similarly able to regulate YAP independent of Hippo signaling (see fig. 6C). While the SRC and mTORC2 phosphorylation sites span the residues of the transcriptional activation domain within YAP, it is possible that these phosphorylation events induce similar conformational states capable of affecting multiple properties of the protein.

YAP and mTOR signaling have been demonstrated to promote GBM proliferation, motility and invasiveness [47]. YAP is overexpressed in glioblastoma and infiltrating gliomas, as well as other CNS tumor types [48,49]. YAP expression has been additionally investigated in four molecular glioblastoma subtypes (classical, mesenchymal, proneural, and neural) and upregulated expression of YAP1 was found in aggressive glioblastoma

Table 1

Relative protein levels of phospho-S^{473}AKT, phospho-S^{436}-YAP1, YAP1, CTGF and Cyr61 in normal and glioblastoma samples.

Samples	pS473-AKT expression§	pS436-YAP1 expression#	YAP expression¥	CTGF expression¬	Cyr61 expression≠
Normal					
1	1.9	1.1	1.5	1.9	2.1
2	1.6	1.3	1.7	2.2	1.7
3	1.1	1.8	1.3	1.3	1.3
4	1.5	1.2	1.4	1.6	1.5
5	1.4	1.6	1.5	1.4	1.9
6	1.7	1.1	1.7	1.8	1.6
GBM					
1	41.3*++	29.4^++	32.4"++	22.6<++	24.8«++
2	64.3*++	32.6^+	29.7"++	21.2<++	14.6«+
3	2.5	10.7^++	1.1	9.4	21.2«++
4	46.1*++	36.4^++	43.2"++	26.9<++	23.5«++
5	17.6*+	22.4^++	55.3"++	33.7<++	19.5«+
6	2.3	5.8	1.9	2.7	2.8
7	46.8*++	12.7^++	45.8"++	16.8<+	33.7«++
8	4.8	6.6	5.8	1.8	2.7
9	7.2	12.4^+	25.4"++	19.3<+	5.2
10	7.9	8.7	46.9"++	11.4<+	11.4«+
11	2.7	2.1	4.7	3.7	4.9
12	39.1*++	42.3^++	49.8"++	29.5<++	33.1«++
13	26.9*++	33.8^++	47.4"++	30.2<<++	16.4«+
14	47.9*++	24.9^++	38.9"++	35.5<++	19.4«+
15	36.8*++	19.5^++	37.2"++	31.6<++	28.6«++
16	52.1*++	40.3	22.7"++	29.4<++	17.5«+
17	3.1	4.8	13.7"+	10.2<+	1.7
18	26.3*++	55.1^++	38.5"++	29.7<++	28.4«++
19	35.7*++	46.2^++	57.1"++	27.8<++	16.9«+
20	15.9*+	34.7^++	29.8"++	25.3<++	20.4«++
21	45.2*++	21.7^++	11.9"+	19.6<+	2.2
22	56.6*	28.3^++	42.6"++	38.7<++	32.2«++
23	2.5	11.7^+	3.4	9.4	4.8
24	6.1	9.2	6.9	12.5<+	16.4«+
25	34.1*++	46.8^++	31.9"++	16.7<+	26.2«++
26	39.4*++	27.9^++	31.5"++	19.2<+	19.7«+
27	9.3	2.2	1.9	8.4	1.1

Note: Six normal brain and twenty-seven independent quick-frozen GBM samples were assessed for phosphorylated AKT, phosphorylated YAP1, total YAP1, CTFG and Cyr61 expression by Western analyses as described in the Materials & Methods section and quantified by densitometry.

17 of 27 tumor samples (63%) had markedly higher mTORC2 activity as determined by monitoring expression levels of phospho-S^{473}-AKT relative to normal brain.

§ phospho-S^{473}-AKT expression > 2-fold above mean of normal brain.

* Markedly increased mTORC2 activity; ++ > 20-fold increase above mean of normal brain (dark gray shaded row); + > 10-fold increase above mean of normal brain (light gray shaded row).

phospho-S^{436}-AKT expression > 2-fold above mean of normal brain.

^ Markedly increased phospho-S^{436}-AKT expression; ++ > 20-fold increase above mean of normal brain + > 10-fold increase above mean of normal brain

¥ YAP expression > 2-fold above mean of normal brain

" Markedly increased YAP expression; ++ > 20-fold increase above mean of normal brain + > 10-fold increase above mean of normal brain

¬ CTGF expression > 2-fold above mean of normal brain.

< Markedly increased CTGF expression; ++ > 20-fold increase above mean of normal brain + > 10-fold increase above mean of normal brain.

≠ Cyr61 expression > 2-fold above mean of normal brain.

« Markedly increased Cyr61 expression; ++ > 20-fold increase above mean of normal brain + > 10-fold increase above mean of normal brain.

subtypes associated with the poorest survival [18]. Merlin, the product of the NF2 gene, has been demonstrated to regulate tissue growth via YAP1 and has been shown to inhibit glioma proliferation and sensitize gliomas to irradiation and chemotherapy [50]. The role of hyperactivated mTORC1 signaling in GBM has been established [1]. mTORC2 signaling has been demonstrated to play an important role in tumor growth, motility, invasiveness, metabolic reprogramming and resistance to targeted therapy in GBM [7,51]. Additionally, mTORC2-mediated regulation of AMOTL2 is required for GBM growth, motility and invasion [27]. Our data demonstrating that direct activation of YAP via mTORC2 further supports the critical roles of the mTORC2 and Hippo signaling pathways in GBM.

In summary, we have characterized a putative phosphorylation site on YAP which when phosphorylated by mTORC2 leads to enhanced, stability, nuclear accumulation, TEAD association and YAP-dependent target gene activity. Mutational analyses demonstrate that phosphorylation of serine 436 promotes YAP-mediated GBM proliferation, motility and invasive characteristics in vitro and in xenograft studies. Experiments utilizing a Hippo pathway resistant YAP mutant suggest that mTORC2 retains the ability to regulate YAP independent of Hippo cascade signaling. It is anticipated that additional mechanisms of cross talk exist between these two fundamental pathways. Delineation of these mechanisms is required for the development of effective targeted therapies.

Abbreviations: mTOR, mechanistic target of rapamycin kinase; mTORC, mechanistic target of rapamycin complex; YAP, Yes-associated protein; TAZ, Transcriptional coactivator with PDZ-binding motif; GBM, glioblastoma multiforme; mLST8, mammalian lethal with SEC13 protein 8; mSin1, mitogen-activated protein kinase-associated protein 1; MEF, mouse embryonic fibroblast; PI3K, phosphatidylinostol 3-kinase; AKT; Protein kinase B; PTEN, Phosphatase and tensin homolog; EGFR, epidermal growth factor receptor; LATS, Large tumor suppressor kinase; AMOT, angiomotin; TEAD, TEA Domain Transcription Factor; TSC1, hamartin; ATG7; Autophagy Related 7; PDX, Patient derived xenograft; STR, short-tandem repeat profiling; siRNA; short-interfering RNA; shRNA, short-hairpin RNA; TRC, The RNAi Consortium; CTGF; connective tissue growth factor; Cyr61; Cysteine-rich angiogenic inducer 61; ANOVA, analysis of variance; AICAR, 5-aminoimidazole-4carboxamide ribonucleoside; Co-IP, co-immunoprecipitation; SRC, tyrosine-protein kinase Src; MK5, MAP kinase-activated protein kinase 5; NF2; Merlin

Author Contributions

Conceptualization, B.H., R.N.N. and J.G.; methodology, A.B.-S., J.T.S., B.H., S.K. and J.G.; investigation, A.B.-S., J.T.S. and B.H.; data curation, A.B.-S., J.T.S., B.H. and J.G.; writing—original draft preparation, B.H. and J.G.; writing—review and editing, B.H., R.N.N., and J.G.; supervision, R.N.N. and J.G.; funding acquisition, J.G. All authors have read and agreed to the published version of the manuscript.

Acknowledgements

We thank Drs. Paul Mischel, Jan Sarkaria, Bing Su, Kun-Liang Guan, David Sabatini, John Ohlfest, Jie Chen, Taekjip Ha and Barry Gumbiner for cell lines and reagents. We thank Dr. Jessie Zhang for assistance with generation and purification of the phospho-S^{436} YAP1 antibody.

Supplementary materials

Supplementary material associated with this article can be found, in the online version, at doi:10.1016/j.neo.2021.07.005.

References

[1] Cloughesy TF, Cavenee WK, Mischel PS. Glioblastoma: from molecular pathology to targeted treatment. *Annu Rev Pathol-Mech* 2014;**9**:1–25.

[2] Prados MD, Byron SA, Tran NL, Phillips JJ, Molinaro AM, Ligon KL, Wen PY, Kuhn JG, Mellinghoff IK, de Groot JF, et al. Toward precision medicine in glioblastoma: the promise and the challenges. *Neuro-oncol* 2015;**17**:1051–63.

3 Cheng H, Zou Y, Ross JS, Wang K, Liu X, Halmos B, Ali SM, Liu H, Verma A, Montagna C, et al. RICTOR Amplification defines a novel subset of patients with lung cancer who may benefit from treatment with mTORC1/2 inhibitors. *Cancer Discov* 2015;**5**:1262–70.

[4] Bashir T, Cloninger C, Artinian N, Anderson L, Bernath A, Holmes B, Benavides-Serrato A, Sabha N, Nishimura RN, Guha A, et al. Conditional astroglial Rictor overexpression induces malignant glioma in mice. *PLoS One* 2012;**7**:e47741.

[5] Driscoll DR, Karim SA, Sano M, Gay DM, Jacob W, Yu J, Mizukami Y, Gopinathan A, Jodrell DI, Evans TR, et al. mTORC2 Signaling drives the development and progression of pancreatic cancer. *Cancer Res* 2016;**76**:6911–23.

[6] Gibault L, Ferreira C, Perot G, Audebourg A, Chibon F, Bonnin S, Lagarde P, Vacher-Lavenu MC, Terrier P, Coindre JM, et al. From PTEN loss of expression to RICTOR role in smooth muscle differentiation: complex involvement of the mTOR pathway in leiomyosarcomas and pleomorphic sarcomas. *Mod Pathol* 2012;**25**:197–211.

[7] Masri J, Bernath A, Martin J, Jo OD, Vartanian R, Funk A, Gera J. mTORC2 activity is elevated in gliomas and promotes growth and cell motility via overexpression of rictor. *Cancer Res* 2007;**67**:11712–20.

[8] Wu SH, Bi JF, Cloughesy T, Cavenee WK, Mischel PS. Emerging function of mTORC2 as a core regulator in glioblastoma: metabolic reprogramming and drug resistance. *Cancer biol med* 2014;**11**:255–63.

[9] Laplante M, Sabatini DM. mTOR signaling in growth control and disease. *Cell* 2012;**149**:274–93.

[10] Oh WJ, Jacinto E. mTOR complex 2 signaling and functions. *Cell cycle (Georgetown, Tex)* 2011;**10**:2305–16.

[11] Oh WJ, Wu CC, Kim SJ, Facchinetti V, Julien LA, Finlan M, Roux PP, Su B, Jacinto E. mTORC2 can associate with ribosomes to promote cotranslational phosphorylation and stability of nascent Akt polypeptide. *EMBO J* 2010;**29**:3939–51.

[12] Zinzalla V, Stracka D, Oppliger W, Hall MN. Activation of mTORC2 by association with the ribosome. *Cell* 2011;**144**:757–68.

[13] Sarbassov DD, Guertin DA, Ali SM, Sabatini DM. Phosphorylation and regulation of Akt/PKB by the rictor-mTOR complex. *Science* 2005;**307**:1098–101.

[14] Tanaka K, Babic I, Nathanson D, Akhavan D, Guo D, Gini B, Dang J, Zhu S, Yang H, De Jesus J, et al. Oncogenic EGFR signaling activates an mTORC2-NF-kappaB pathway that promotes chemotherapy resistance. *Cancer Discov* 2011;**1**:524–38.

[15] Read RD, Fenton TR, Gomez GG, Wykosky J, Vandenberg SR, Babic I, Iwanami A, Yang H, Cavenee WK, Mischel PS, et al. A kinome-wide RNAi screen in Drosophila Glia reveals that the RIO kinases mediate cell proliferation and survival through TORC2-Akt signaling in glioblastoma. *PLos Genet* 2013;**9**:e1003253.

[16] Yu FX, Zhao B, Guan KL. Hippo pathway in organ size control, tissue homeostasis, and cancer. *Cell* 2015;**163**:811–28.

[17] Bhat KP, Salazar KL, Balasubramaniyan V, Wani K, Heathcock L, Hollingsworth F, James JD, Gumin J, Diefes KL, Kim SH, et al. The transcriptional coactivator TAZ regulates mesenchymal differentiation in malignant glioma. *Genes Dev* 2011;**25**:2594–609.

[18] Orr BA, Bai H, Odia Y, Jain D, Anders RA, Eberhart CG. Yes-associated protein 1 is widely expressed in human brain tumors and promotes glioblastoma growth. *J Neuropathol Exp Neurol* 2011;**70**:568–77.

[19] Meng Z, Moroishi T, Guan KL. Mechanisms of Hippo pathway regulation. *Genes Dev* 2016;**30**:1–17.

[20] Yu FX, Guan KL. The Hippo pathway: regulators and regulations. *Genes Dev* 2013;**27**:355–71.

[21] Zhao B, Li L, Lu Q, Wang LH, Liu CY, Lei Q, Guan KL. Angiomotin is a novel Hippo pathway component that inhibits YAP oncoprotein. *Genes Dev* 2011;**25**:51–63.

[22] Totaro A, Panciera T, Piccolo S. YAP/TAZ upstream signals and downstream responses. *Nat Cell Biol* 2018;**20**:888–99.

[23] Betz C, Hall MN. Where is mTOR and what is it doing there? *J Cell Biol* 2013;**203**:563–74.

[24] Tumaneng K, Schlegelmilch K, Russell RC, Yimlamai D, Basnet H, Mahadevan N, Fitamant J, Bardeesy N, Camargo FD, Guan KL. YAP mediates crosstalk between the Hippo and PI(3)K-TOR pathways by suppressing PTEN via miR-29. *Nat Cell Biol* 2012;**14**:1322–9.

[25] Yu FX, Zhao B, Panupinthu N, Jewell JL, Lian I, Wang LH, Zhao J, Yuan H, Tumaneng K, Li H, et al. Regulation of the Hippo-YAP pathway by G-protein-coupled receptor signaling. *Cell* 2012;**150**:780–91.

[26] Mo JS, Yu FX, Gong R, Brown JH, Guan KL. Regulation of the hippo-YAP pathway by protease-activated receptors (PARs). *Gene Dev* 2012;**26**:2138–43.

[27] Artinian N, Cloninger C, Holmes B, Benavides-Serrato A, Bashir T, Gera J. Phosphorylation of the hippo pathway component AMOTL2 by the mTORC2 Kinase promotes yap signaling, resulting in enhanced glioblastoma growth and invasiveness. *J Biol Chem* 2015;**290**:19387–401.

[28] Gera JF, Hazbun TR, Fields S. Array-based methods for identifying protein-protein and protein-nucleic acid interactions. *Method Enzymol* 2002;**350**:499–512.

[29] Hara K, Maruki Y, Long XM, Yoshino K, Oshiro N, Hidayat S, Tokunaga C, Avruch J, Yonezawa K. Raptor, a binding partner of target of rapamycin (TOR), mediates TOR action. *Cell* 2002;**110**:177–89.

[30] Brown MC, Gromeier M. MNK Controls mTORC1: Substrate Association through Regulation of TELO2 Binding with mTORC1. *Cell Rep* 2017;**18**:1444–57.

[31] Kim NG, Gumbiner BM. Adhesion to fibronectin regulates Hippo signaling via the FAK-Src-PI3K pathway. *J Cell Biol* 2015;**210**:503–15.

[32] Dignam JD, Lebovitz RM, Roeder RG. Accurate transcription initiation by rna polymerase-ii in a soluble extract from isolated mammalian nuclei. *Nucleic Acids Res* 1983;**11**:1475–89.

[33] Holmes B, Lee J, Landon KA, Benavides-Serrato A, Bashir T, Jung ME, Lichtenstein A, Gera J. Mechanistic target of rapamycin (MTOR) inhibition synergizes with reduced internal ribosome entry site (IRES)-mediated translation of Cyclin D1 and c-MYC mRNAs to treat glioblastoma. *J Biol Chem* 2016;**291**:14146–59.

[34] Gui Y, Li JZ, Lu QM, Feng Y, Wang MJ, He WC, Yang JW, Dai CS. Yap/Taz mediates mTORC2-stimulated fibroblast activation and kidney fibrosis. *J Biol Chem* 2018;**293**:16364–75.

[35] Cameron AJM, Linch MD, Saurin AT, Escribano C, Parker PJ. mTORC2 targets AGC kinases through Sin1-dependent recruitment. *Biochem J* 2011;**439**:287–97.

[36] Kazyken D, Magnuson B, Bodur C, Acosta-Jaquez HA, Zhang DQ, Tong X, Barnes TM, Steinl GK, Patterson NE, Altheim CH, et al. AMPK directly activates mTORC2 to promote cell survival during acute energetic stress. *Sci Signal* 2019;**12**.

[37] Masui K, Tanaka K, Ikegami S, Villa GR, Yang HJ, Yong WH, Cloughesy TF, Yamagata K, Arai N, Cavenee WK, et al. Glucose-dependent acetylation of Rictor promotes targeted cancer therapy resistance. *P Natl Acad Sci USA* 2015;**112**:9406–11.

[38] Benavides-Serrato A, Lee J, Holmes B, Landon KA, Bashir T, Jung ME, Lichtenstein A, Gera J. Specific blockade of Rictor-mTOR association inhibits mTORC2 activity and is cytotoxic in glioblastoma (vol 12, e0176599, 2017). *PLoS One* 2019;**14**:e0212160.

[39] Ruan C, Ouyang XX, Liu HZ, Li S, Jin JS, Tang WY, Xia Y, Su B. Sin1-mediated mTOR signaling in cell growth, metabolism and immune response. *Natl Sci Rev* 2019;**6**:1149–62.

[40] Basu S, Totty NF, Irwin MS, Sudol M, Downward J. Akt phosphorylates the Yes-associated protein, YAP, to induce interaction with 14-3-3 and attenuation of p73-mediated apoptosis. *Mol Cell* 2003;**11**:11–23.

[41] Masliantsev K, Karayan-Tapon L, Guichet PO. Hippo signaling pathway in gliomas. *Cells-Basel* 2021;**10**.

[42] Shimobayashi M, Hall MN. Making new contacts: the mTOR network in metabolism and signalling crosstalk. *Nat Rev Mol Cell Bio* 2014;**15**:155–62.

[43] Zhao B, Wei X, Li W, Udan RS, Yang Q, Kim J, Xie J, Ikenoue T, Yu J, Li L, et al. Inactivation of YAP oncoprotein by the Hippo pathway is involved in cell contact inhibition and tissue growth control. *Gene Dev* 2007;**21**:2747–61.

[44] Lamar JM, Xiao YX, Norton E, Jiang ZG, Gerhard GM, Kooner S, Warren JSA, Hynes RO. SRC tyrosine kinase activates the YAP/TAZ axis and thereby drives tumor growth and metastasis. *J Biol Chem* 2019;**294**:2302–17.

[45] Li P, Silvis MR, Honaker Y, Lien WH, ST Arron, Vasioukhin V. alpha E-catenin inhibits a Src-YAP1 oncogenic module that couples tyrosine kinases and the effector of Hippo signaling pathway. *Gene Dev* 2016;**30**:798–811.

46 Seo J, Kim MH, Hong H, Cho H, Park S, Kim SK, Kim J. MK5 regulates YAP stability and is a molecular target in YAP-driven cancers. *Cancer Res* 2019;**79**:6139–52.

[47] Liu YC, Wang YZ. Role of Yes-associated protein 1 in gliomas: pathologic and therapeutic aspects. *Tumor Biol* 2015;**36**:2223–7.

[48] Fernandez A, Squatrito M, Northcott P, Awan A, Holland EC, Taylor MD, Nahle Z, Kenney AM. Oncogenic YAP promotes radioresistance and genomic instability in medulloblastoma through IGF2-mediated Akt activation. *Oncogene* 2012;**31**:1923–37.

[49] Modena P, Lualdi E, Facchinetti F, Veltman J, Reid JF, Minardi S, Janssen I, Giangaspero F, Forni M, Finocchiaro G, et al. Identification of tumor-specific molecular signatures in intracranial ependymoma and association with clinical characteristics. *J Clin Oncol* 2006;**24**:5223–33.

[50] Lau YKI, Murray LB, Houshmandi SS, Xu Y, Gutmann DH, Yu Q. Merlin is apotent inhibitor of glioma growth. *Cancer Res* 2008;**68**:5733–42.

[51] Masui K, Cavenee WK, Mischel PS. mTORC2 and metabolic reprogramming in GBM: at the interface of genetics and environment. *Brain Pathol* 2015;**25**:755–9.